

Two-loop QCD corrections to the $V \rightarrow q\bar{q}g$ helicity amplitudes with axial-vector couplings

Thomas Gehrmann,^a Tiziano Peraro^b and Lorenzo Tancredi^c

^a*Physik-Institut, Universität Zürich,
Winterthurerstrasse 190, CH-8057 Zürich, Switzerland*

^b*Dipartimento di Fisica e Astronomia, Università di Bologna e INFN, Sezione di Bologna,
via Irnerio 46, I-40126 Bologna, Italy*

^c*Physik Department, Technische Universität München,
James-Franck-Straße 1, D-85748 Garching, Germany*

E-mail: thomas.gehrmann@uzh.ch, tiziano.peraro@unibo.it,
lorenzo.tancredi@tum.de

ABSTRACT: We compute the two-loop corrections to the helicity amplitudes for the coupling of a massive vector boson to a massless quark-antiquark pair and a gluon, accounting for vector and axial-vector couplings of the vector boson and distinguishing isospin non-singlet and singlet contributions. A new four-dimensional basis for the decomposition of the amplitudes into 12 invariant tensor structures is introduced. The associated form factors are then computed up to two loops in QCD using dimensional regularization. After performing renormalization and infrared subtraction, the finite parts of the renormalized non-singlet vector and axial-vector form factors are shown agree with each other, and to reproduce the previously known two-loop amplitudes. The singlet axial-vector amplitude receives a contribution from the axial anomaly from two loops onwards. This amplitude is computed for massless and massive internal quarks. Our results provide the last missing two-loop amplitudes entering the NNLO QCD corrections of vector-boson-plus-jet production at hadron colliders.

KEYWORDS: Higher-Order Perturbative Calculations, Specific QCD Phenomenology

ARXIV EPRINT: [2211.13596](https://arxiv.org/abs/2211.13596)

Contents

1	Introduction	1
2	The tensor decomposition including axial-vector terms	3
3	Calculation of the form factors	7
3.1	Massless two-loop corrections	8
3.2	Massive two-loop corrections	9
3.2.1	The unrenormalised form factors up to two loops	11
4	UV renormalisation and subtraction of the IR poles	12
5	The helicity amplitudes	16
5.1	Helicity amplitudes for an external vector and axial-vector current	16
5.2	Helicity amplitudes for a Standard Model vector boson	22
5.3	Checks on the results	24
6	Conclusions	25

1 Introduction

The scattering amplitudes involving a massive electroweak gauge boson and three massless QCD partons enter, in their different kinematical crossings, the theory predictions for important QCD precision observables: $e^+e^- \rightarrow 3$ jets, $ep \rightarrow (2+1)$ jets and $pp \rightarrow V+\text{jet}$.

Especially three-jet production in e^+e^- played an outstanding role in establishing QCD as theory of the strong interaction and in the discovery of the gluon [1]. The quest for a precise theoretical understanding of three-jet production observables [2] demanded higher order perturbative QCD corrections. The one-loop corrections to the $V \rightarrow q\bar{q}g$ amplitudes were computed in the context of the next-to-leading order (NLO) corrections to three-jet production [3, 4], and the two-loop corrections to these amplitudes [5, 6] were first applied in computing the next-to-next-to-leading order (NNLO) corrections to this process [7–10]. Crossings of the scattering amplitudes to the other processes were then obtained by analytic continuation [11, 12] to the relevant kinematical regions.

Beyond tree-level, one can separate the $V \rightarrow q\bar{q}g$ amplitudes by an isospin projection on the external quarks into non-singlet contributions (where the gauge boson couples to the spin line of the external quark) and pure-singlet contributions (where the gauge boson couples to a closed quark loop unrelated to the external quark spin line). Example diagrams are shown in figure 1. The pure-singlet contributions vanish trivially for $V = W^\pm$ due to charge conservation.

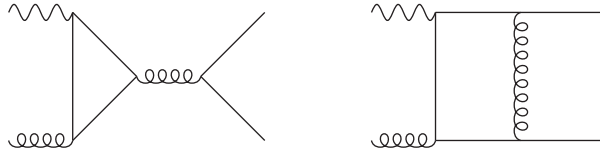


Figure 1. Example of Feynman diagrams for singlet (left) and non-singlet (right) contributions.

The coupling structure of the external vector boson to quarks involves a vector and an axial-vector component. For massless external quarks, one expects the non-singlet contributions to the vector and axial-vector $V \rightarrow q\bar{q}g$ amplitudes to agree due to chirality conservation of massless fermions. Owing to the conceptual difficulty of handling axial-vector currents in dimensional regularization, this agreement has however never been checked explicitly beyond tree level.

The pure-singlet contribution at one loop vanishes for a vector coupling. For an axial-vector coupling, one finds a finite one-loop amplitude [13, 14], which vanishes if the internal quark flavours are summed over a mass-degenerate isospin doublet. Consequently, the large mass splitting between top and bottom quarks in the third generation results in a non-vanishing pure-singlet axial-vector contribution. The one-loop pure-singlet axial-vector amplitude is finite for internal massless quarks q' , and suppressed as $(m_{Q'}/m_V)^2$ in the large mass limit of the internal quark Q' . At two loops, the pure-singlet contribution was computed up to now only for a vector coupling [5, 6].

Most jet observables in e^+e^- average over the incoming beam direction. In this case, the pure-singlet axial-vector contribution averages out to zero. Its contribution to jet production in ep collisions is strongly suppressed by the Z boson mass. In Z +jet production, the numerical magnitude of the one-loop pure-singlet axial-vector contribution was found to be very small (per-mille correction) for sufficiently inclusive observables [13], but potentially becomes sizable in specific angular correlations between the jet and the decay lepton momenta [15].

Up to now, all NNLO QCD calculations of Z +jet production at the LHC [16–18] discarded the axial-vector pure-singlet contributions, due to the lack of the corresponding two-loop axial-vector amplitudes for crossings of $Z \rightarrow q\bar{q}g$. At the same level, other axial-vector pure-singlet contributions to Z +jet production are known [19–21], but could not be included consistently up to now. The very same axial-vector pure-singlet amplitudes also contribute to the third-order (N3LO) corrections to Z boson production at hadron colliders. Their contribution to the inclusive Z boson coefficient functions at N3LO has been computed most recently [22] by combining loop and phase space integrations.

It is the purpose of the current paper to complete the two-loop helicity amplitudes for $Z \rightarrow q\bar{q}g$ by explicitly establishing the identity of vector and axial-vector non-singlet amplitudes and by computing the missing pure-singlet axial-vector amplitudes for massless and very massive internal quarks. This paper is structured as follows: in section 2, we describe a novel four-dimensional tensor decomposition of the helicity amplitudes and introduce projectors on the relevant form factors, which are then computed in section 3.

Their renormalization and infrared factorization is described in section 4. The form factors are then assembled into the helicity amplitudes for $Z \rightarrow q\bar{q}g$ in section 5. We conclude with an outlook in section 6.

2 The tensor decomposition including axial-vector terms

We consider the decay of a space-like electroweak gauge boson to a pair of quarks and a gluon up to two loops in QCD. We work in massless QCD assuming $N_f = 5$ massless quarks. When evaluated for a single quark flavour, the axial-vector pure-singlet contribution contains an axial anomaly, which is cancelled upon summation over both quark flavours in an isospin doublet. To obtain a consistent result, we also allow top quarks in the virtual loops of the axial-vector pure-singlet contribution (and only in this contribution), which we compute in the limit of infinitely large top-mass $m_t \rightarrow \infty$. As a byproduct of our calculation, we also recompute the well-known non-singlet contributions, limiting ourselves in that case to consider only massless quarks circulating in the loops.

The full electroweak Standard Model couplings are inserted only in section 5 when assembling the helicity amplitudes. For their tensor decomposition and the subsequent calculation of the corresponding form factors, we instead consider QCD coupled to an external vector or axial-vector current with unit coupling constant. The vector current is conserved to all orders in perturbation theory, and in any number of dimensions. The pure-singlet axial-vector current is anomalous and requires renormalization (which cancels out upon summation over a quark isospin doublet). The conservation of the non-singlet axial-vector current is broken by dimensional regularisation and has to be restored by a finite renormalization. The renormalization of axial-vector currents in QCD is described in detail in section 4 below.

For definiteness, we work in the decay kinematics

$$V(p_4) \rightarrow \bar{q}(p_1) + q(p_2) + g(p_3),$$

from which the relevant scattering channels can be obtained by crossing symmetry and a corresponding analytic continuation [12]. To parametrise the kinematics of this scattering process, we recall that

$$p_1^2 = p_2^2 = p_3^2 = 0, \quad p_4^2 = (p_1 + p_2 + p_3)^2 = q^2,$$

and introduce the usual Mandelstam invariants, defined in the decay kinematics as

$$s_{12} = (p_1 + p_2)^2, \quad s_{13} = (p_1 + p_3)^2, \quad s_{23} = (p_2 + p_3)^2, \quad s_{12} + s_{13} + s_{23} = q^2. \quad (2.1)$$

Note that for generality we use q^2 for the invariant mass of the vector boson. For later convenience, following [23, 24] we also introduce the three dimensionless ratios

$$x = \frac{s_{12}}{q^2}, \quad y = \frac{s_{13}}{q^2}, \quad z = \frac{s_{23}}{q^2}, \quad \text{with } x + y + z = 1. \quad (2.2)$$

In terms of any pair of the variables above, say y, z , the decay kinematics is mapped by

$$0 < y < 1, \quad 0 < z < 1 - y.$$

A possible approach to the computation of multi-loop amplitudes starts with their decomposition into a basis of independent Lorentz tensor structures, from which one can then extract the so-called helicity amplitudes. Our starting point here is the construction described in [25, 26], which makes it possible to avoid the calculation of evanescent tensor structures in $d = 4$ space-time dimensions. As we will see, this is particularly convenient in the presence of an axial coupling. A nice aspect of this construction is also that the number of independent tensor structures always matches one-to-one the number of independent helicity amplitudes in $d = 4$.

In the process under consideration helicity conservation along the massless external fermion line implies that there can be $2 \times 2 \times 3 = 12$ independent helicity configurations: 2 for the quark line, 2 for the on-shell gluon and 3 for the off-shell vector boson V . In the absence of parity breaking terms, these would be reduced to 6 by the trivial transformation properties of the helicity amplitudes of a $2 \rightarrow 2$ scattering process under parity. As explained in [25], this reduction no longer takes place starting for five or more external particles, since the helicity amplitudes in that case depend explicitly on the parity-breaking object $\text{tr}_5 = \epsilon^{p_1 p_2 p_3 p_4}$. Clearly, if the vector boson couples chirally as a Standard Model Z or W boson, this simplification does not occur and we expect a total of 12 independent tensor structures to be required to fully decompose both vector and axial-vector parts of the scattering amplitude.

As it was shown in [25, 26], by working in the 't Hooft-Veltman dimensional regularisation scheme [27], we can limit ourselves to perform a tensor decomposition assuming that all external states are in exactly $d = 4$ space-time dimensions, since all remaining evanescent tensor structures turn out not to contribute to the helicity amplitudes, even in $d = 4 - 2\epsilon$. To construct the tensor decomposition for our problem, a convenient starting point is a basis of four independent vectors in $d = 4$. The first three vectors can be chosen to be the three independent momenta $p_1^\mu, p_2^\mu, p_3^\mu$, such that the natural fourth independent vector is the orthogonal, axial-vector

$$\epsilon^{\nu\rho\sigma\mu} p_{1\nu} p_{2\rho} p_{3\sigma} = \epsilon^{p_1 p_2 p_3 \mu} = v_A^\mu, \tag{2.3}$$

where $\epsilon^{\mu\nu\rho\sigma}$ is the Levi-Civita symbol, defined using FORM conventions that correspond to

$$\epsilon^{0123} = -\epsilon_{0123} = -i, \quad \epsilon^{\mu\nu\rho\sigma} \epsilon_{\mu\nu\rho\sigma} = 24 + \mathcal{O}(d-4). \tag{2.4}$$

We stress here that $p_i \cdot v_A = 0$.

Note also that, by using $q_i^\mu = \{p_1^\mu, p_2^\mu, p_3^\mu, v_A^\mu\}$ as independent vectors, we do not need to include in our tensor decomposition neither $g^{\mu\nu}$ nor other higher-rank tensors obtained from the Levi-Civita tensor as $\epsilon^{p_i p_j \mu\nu}$ for $i, j = 1, 2, 3$, since in $d = 4$ they are not linearly independent from all tensors built from the q_i^μ . A crucial point here, since we are dealing with external fermions, is that the same is true also for the Dirac γ^μ , and we have

$$\gamma^\mu = \sum_{i=1}^4 \hat{a}_i q_i^\mu, \quad g^{\mu\nu} = \sum_{i,j=1}^4 b_{ij} q_i^\mu q_j^\nu, \quad \epsilon^{p_k p_l \mu\nu} = \sum_{i,j=1}^4 c_{ij}^{(kl)} q_i^\mu q_j^\nu, \tag{2.5}$$

where clearly the coefficients b_{ij} and $c_{ij}^{(kl)}$ are scalar functions while \hat{a}_i must be linear combinations of $q_i = q_i^\mu \gamma_\mu$. Their exact form does not matter for what follows.

With these observations, and assuming that helicity is conserved along the fermion line, the amplitude can be easily decomposed in independent tensors. We start by defining

$$\mathcal{M} = -i \sqrt{4\pi\bar{\alpha}_s} \mathbb{T}_{ij}^a \epsilon_{4,\mu} \epsilon_{3,\nu} A^{\mu\nu} \quad (2.6)$$

where $\bar{\alpha}_s$ is the bare strong coupling and \mathbb{T}_{ij}^a are the SU(3) color fundamental generators. The external vector or axial-vector vertex does not carry a coupling constant. The rank-two tensor can be decomposed as

$$\begin{aligned} A^{\mu\nu} = & \bar{u}(p_2) \not{p}_3 u(p_1) \left[\tilde{F}_1 p_1^\mu p_1^\nu + \tilde{F}_2 p_2^\mu p_1^\nu + \tilde{F}_3 v_A^\mu v_A^\nu + \tilde{G}_1 p_1^\mu v_A^\nu + \tilde{G}_2 p_2^\mu v_A^\nu + \tilde{G}_3 v_A^\mu p_1^\nu \right] \\ & + \bar{u}(p_2) \not{p}_A u(p_1) \left[\tilde{F}_4 p_1^\mu v_A^\nu + \tilde{F}_5 p_2^\mu v_A^\nu + \tilde{F}_6 v_A^\mu p_1^\nu + \tilde{G}_4 p_1^\mu p_1^\nu + \tilde{G}_5 p_2^\mu p_1^\nu + \tilde{G}_6 v_A^\mu v_A^\nu \right], \end{aligned} \quad (2.7)$$

where \tilde{F}_i and \tilde{G}_i are scalar form factors. In order to obtain (2.7), we also used the transversality condition for the external gluon

$$\epsilon_3 \cdot p_3 = 0,$$

together with the following gauge choices for the gluon and the off-shell vector boson

$$\epsilon_3 \cdot p_2 = 0, \quad \epsilon_4 \cdot p_4 = 0 \quad (\text{Lorenz Gauge}).$$

We stress that this gauge choice implies the following polarisation sums rules

$$\sum_{pol} \epsilon_3^{\mu*} \epsilon_3^\nu = -g^{\mu\nu} + \frac{p_3^\mu p_2^\nu + p_3^\nu p_2^\mu}{p_2 \cdot p_3}, \quad \sum_{pol} \epsilon_4^{\mu*} \epsilon_4^\nu = -g^{\mu\nu} + \frac{p_4^\mu p_4^\nu}{q^2}. \quad (2.8)$$

While fixing the gauge is not necessary in principle, it provides a clear way to enumerate all independent structures.

Looking again at (2.7), we see that by using the vector v_A^μ , we generate exactly 12 independent tensors in $d = 4$ dimensions, which conveniently separate into 6 parity-even (\tilde{F}_i) and 6 parity-odd (\tilde{G}_i) structures. We stress once more that this simple separation is only possible for the scattering of up to 4 particles.

Starting from (2.7), we can obtain an alternative decomposition, that has the advantage of involving at most one occurrence of the parity-odd vector v_A^μ , only in those tensors that are parity-violating. This is particularly useful to get rid of the possible ambiguity in the order of contraction of pairs of Levi-Civita tensors when we define the corresponding projectors and apply them on the amplitude using Larin scheme [28]. Starting from the fact that $g^{\mu\nu}$ is parity-even (and can thus contains only products of an even number of v_A^μ), we can write

$$g^{\mu\nu} = \sum_{i,j=1}^3 b_{ij} p_i^\mu p_j^\nu + b v_A^\mu v_A^\nu,$$

and we easily see that we can effectively substitute $v_A^\mu v_A^\nu \sim g^{\mu\nu}$ everywhere in the tensor decomposition, still spanning the same vector space. This provides the alternative

tensor decomposition

$$\begin{aligned}
 A^{\mu\nu} = & \bar{u}(p_2)\not{p}_3 u(p_1) \left[F_1 p_1^\mu p_1^\nu + F_2 p_2^\mu p_1^\nu + F_3 g^{\mu\nu} + G_1 p_1^\mu v_A^\nu + G_2 p_2^\mu v_A^\nu + G_3 v_A^\mu p_1^\nu \right] \\
 & + \bar{u}(p_2)\gamma^\nu u(p_1) \left[F_4 p_1^\mu + F_5 p_2^\mu \right] + \bar{u}(p_2)\gamma^\mu u(p_1) F_6 p_1^\nu \\
 & + \bar{u}(p_2)\not{p}_A u(p_1) \left[G_4 p_1^\mu p_1^\nu + G_5 p_2^\mu p_1^\nu \right] + G_6 \left[\bar{u}(p_2)\gamma^\mu u(p_1)v_A^\nu + \bar{u}(p_2)\gamma^\nu u(p_1)v_A^\mu \right],
 \end{aligned} \tag{2.9}$$

in terms of new form factors F_i and G_j . The choice made for the tensor multiplying form factor G_6 deserves special attention. Indeed, there would be three equivalent choices to substitute $v_A^\mu v_A^\nu$

$$\bar{u}(p_2)\not{p}_A u(p_1)v_A^\mu v_A^\nu \rightarrow \begin{cases} \bar{u}(p_2)\not{p}_A u(p_1)g^{\mu\nu} \\ \bar{u}(p_2)\gamma^\mu u(p_1)v_A^\nu \\ \bar{u}(p_2)\gamma^\nu u(p_1)v_A^\mu \end{cases},$$

and the last two can be rearranged into their symmetric combination

$$\bar{u}(p_2)\not{p}_A u(p_1)v_A^\mu v_A^\nu \rightarrow \bar{u}(p_2)\gamma^\mu u(p_1)v_A^\nu + \bar{u}(p_2)\gamma^\nu u(p_1)v_A^\mu. \tag{2.10}$$

We chose this last option in (2.9) as the most natural one in the 't Hooft-Veltman scheme, as we will elaborate upon in section 3.2.1 below.

We rewrite (2.9) formally as

$$A^{\mu\nu} = \sum_{i=1}^6 F_i T_i^{E,\mu\nu} + \sum_{i=1}^6 G_i T_i^{O,\mu\nu}, \tag{2.11}$$

where the identification of the parity-even ($T_j^{E,\mu\nu}$) and parity-odd ($T_j^{O,\mu\nu}$) tensors is obvious comparing with (2.9).

The newly defined 12 tensors should be thought of as vectors in a vector space endowed with the scalar product defined by

$$T_i^{P_1\dagger} \cdot T_j^{P_2} = T_i^{P_1,\mu_1\nu_1\dagger} \kappa_{\mu_1\mu_2\nu_1\nu_2} T_j^{P_2,\mu_2\nu_2} \tag{2.12}$$

where $P_i = \{E, O\}$ and the metric reads

$$\kappa^{\mu_1\mu_2\nu_1\nu_2} = \left(-g^{\mu_1\mu_2} + \frac{p_4^{\mu_1} p_4^{\mu_2}}{q^2} \right) \left(-g^{\nu_1\nu_2} + \frac{p_3^{\nu_1} p_2^{\nu_2} + p_3^{\nu_2} p_2^{\nu_1}}{p_2 \cdot p_3} \right). \tag{2.13}$$

This definition implements the gauge choice imposed on the external vector bosons. With this scalar product it is easy to see that even and odd tensors are mutually orthogonal

$$T_i^{E\dagger} \cdot T_j^O = T_i^{O\dagger} \cdot T_j^E = 0. \tag{2.14}$$

An important point should be stressed here: the decomposition in (2.9) should not be interpreted as a purely four-dimensional decomposition, but instead as a decomposition valid in the 't Hooft-Veltman scheme. This means that when we perform the sums in (2.12), indices

that are not explicitly contracted with external momenta are taken to be d -dimensional. This implies, in particular, that we use consistently throughout the calculation

$$g^{\mu\nu}g_{\mu\nu} = d, \quad v_A \cdot v_A = \frac{d-3}{4}s_{12}s_{13}s_{23}. \quad (2.15)$$

We stress here, to avoid a possible source of confusion with the Levi-Civita tensor, that when we take the adjoint of the tensors, we *do not* complex conjugate the vector v_A .

Thanks to the orthogonality of the two sets of tensors, we can define two independent sets of *projector operators* \mathcal{P}_i^P , which are suitable vectors in the dual vector space defined such that

$$\mathcal{P}_i^P \cdot T_j^P = \delta_{ij} \quad \text{for } P = \{E, O\}. \quad (2.16)$$

By expanding the projectors in the same basis of dual vectors

$$\mathcal{P}_i^P = \sum_{j=1}^6 c_j^{(i),P} T_j^{P\dagger}, \quad (2.17)$$

their coefficients $c_j^{(i),P}$ can be obtained by inverting the matrix $(M^P)_{nm} = T_n^{P\dagger} \cdot T_m^P$ as

$$c_j^{(i),P} = \left(M^P\right)_{ij}^{-1}. \quad (2.18)$$

We provide algebraic expressions for the projectors as supplementary material attached to this paper.

3 Calculation of the form factors

Once the projector operators have been defined, it is conceptually straightforward to apply them on a representation for the scattering amplitude in terms of Feynman diagrams. Our calculation proceeds here in a rather standard way: we produce all relevant diagrams at tree level, one loop and two loops with QGRAF [29] and perform the necessary manipulations which follow from the application of the projectors defined in (2.17) in FORM [30]. To deal with γ_5 consistently with our tensor decomposition, we use the Larin-scheme [28], which defines the axial-vector current through the anti-symmetrised replacement

$$\gamma^\mu \gamma^5 \rightarrow \frac{1}{2} \left(\gamma^\mu \gamma^5 - \gamma^5 \gamma^\mu \right) = \frac{1}{6} \epsilon^{\mu\nu\rho\sigma} \gamma_\nu \gamma_\rho \gamma_\sigma. \quad (3.1)$$

Notice that Larin prescription has been adapted to be consistent with our conventions for the Levi-Civita tensor. With this definition, no explicit dimensional splitting is required. Moreover, we see that in this scheme it is straightforward to apply both parity-even and parity-odd projectors on the Feynman diagrams: in fact, parity invariance of the form factors, together with the block-diagonal form of the projector operators, guarantee that the parity-even(odd) projectors only need to be applied on the vector(axial-vector) part of the scattering amplitude. The definition in (3.1), together with the explicit form of the tensors in (2.17), shows that one always has to consider at most the contraction of one pair of Levi-Civita tensors. The contraction can be performed assuming that indices are in general

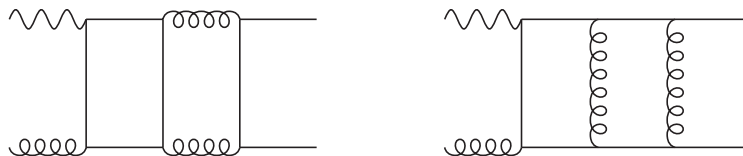


Figure 2. Example of Feynman diagrams for singlet (left) and non-singlet (right) two-loop massless corrections.

d -dimensional and this allows for a straightforward manipulation of the corresponding scalar expressions in dimensional regularisation.

After acting with the projectors on the Feynman diagrams, it is immediate to manipulate all resulting Feynman integrals and map them to integral families. At this point, our treatment of the Feynman diagrams that only contain massless quarks proceeds differently compared to those that involve the exchange of massive top quarks, we therefore discuss the two cases separately below.

3.1 Massless two-loop corrections

As already stated in the previous sections, when computing the massless quark contributions, we consider both a vector and axial-vector interaction and include all relevant Feynman diagrams, including pure-singlet and non-singlet diagrams. While results for the purely vector and for the non-anomalous axial-vector part of the amplitude have already been known in the literature for some time [31], recomputing them in our current setup allows us to perform various consistency checks on the calculation, as it will be explained below.

Up to two loops, all integrals stemming from Feynman diagrams which only involve massless virtual quark exchanges can be easily mapped to the integral families originally defined in [23, 24]. Some examples of the relevant Feynman diagrams are displayed in figure 2.

We observe that, after the projectors are applied to the Feynman diagrams, only scalar integrals up to numerator rank 4 appear in the parity-even form factors, while the parity-odd ones require seven-propagator non-planar integrals up to rank 5. Despite this, the reduction is relatively simple and can be easily performed with standard automated codes. We use Reduze 2 [32, 33], which conveniently includes procedures to map the Feynman diagrams to the relevant integral families (and their crossings), and takes care of removing redundancies among the integrals due to sector symmetries and sector relations, see ref. [33] for details. By using the explicit analytic expressions for the master integrals [23, 24], it is then straightforward to obtain analytic expressions for the *bare* vector and axial-vector form factors up to two-loops in terms of so-called Harmonic Polylogarithms (HPLs) [34] and 2-dimensional Harmonic Polylogarithms (2dHPLs) [23], which can be evaluated numerically [35–37] from their series representations.

In the modern language of multiple polylogarithms, we define 2dHPLs as

$$G(a_1, \dots, a_n; z) = \int_0^z \frac{dx_1}{x_1 - a_1} G(a_2, \dots, a_n; x_1), \quad G(0, \dots, 0; z) = \frac{1}{n!} \log^n z, \\ G(z) = 1, \quad \text{with} \quad a_i = \{-1, 1, 0, -y, 1 - y\}, \quad (3.2)$$

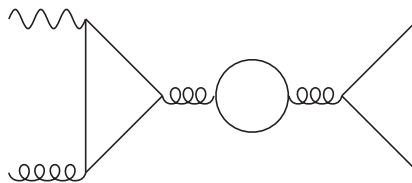


Figure 3. Example of self-energy corrections to the pure-singlet class of diagrams. Both N_f massless and N_h massive quarks are allowed to circulate in all fermion loops.

where for the problem under study, the variables y, z turn out to be any pair of the dimensionless ratios introduced in eqs. (2.2). The symmetry of the kinematical constraints allows one to prove that the same set of functions is sufficient to describe the result for any pair of the variables defined in (2.2). Moreover, it can be shown that by suitably redefined variables, the same is true in all other kinematically relevant crossings, including the scattering kinematics [12], allowing to compute the amplitudes for $q\bar{q} \rightarrow Vg$ and $qg \rightarrow Vq$ in terms of the same class of functions.

3.2 Massive two-loop corrections

We compute the leading contributions arising from massive fermion loops to the two-loop pure-singlet axial-vector amplitudes in the limit of a large top quark mass $m_t \rightarrow \infty$. While the corresponding one-loop amplitudes start at $\mathcal{O}(1/m_t^2)$, at two loops we also have an $\mathcal{O}(1)$ contribution in that limit. While we are mostly interested in this $\mathcal{O}(1)$ contribution, we also include all terms up to $\mathcal{O}(1/m_t^2)$ in our results for the pure-singlet axial amplitudes at one and two loops, which allows us to perform consistency checks of our computational setup and the renormalization and infrared factorization procedure.

We generate the integrands by contracting our twelve projection tensors with the amplitude, keeping the full dependence on the top quark mass. As explained above, we limit ourselves to consider mass corrections to the subset of diagrams which contribute to the pure-singlet amplitude. For consistency, when considering these diagrams we allow massive top quarks also in self-energy corrections, as for example in figure 3. The Feynman integrals in the amplitude are then mapped to two-loop integral families using Reduze 2.

In order to obtain an expansion for large m_t , we employ the strategy of regions [38]. The top quark mass m_t only appears as an internal mass in a closed sub-loop. We first focus on two-loop diagrams with only one massive subloop. There are two non-vanishing integration regions contributing to the limit $m_t \rightarrow \infty$. Let k_1 and k_2 be the two loop momenta. We identify k_2 as the loop momentum running in the fermion loop. Hence, the mass m_t only appears in loop propagators depending on k_2 (or both k_1 and k_2) while propagators depending only on k_1 are massless. The first region, which we henceforth call the *large region*, is the one where all loop momenta are large, i.e. of the same order as m_t ,

$$k_1 = \mathcal{O}(m_t), \quad k_2 = \mathcal{O}(m_t). \tag{3.3}$$

The second region, which we call the *small region*, is the one where the loop momentum k_1

is small compared to m_t , while k_2 is still large,

$$k_1 = \mathcal{O}(1), \quad k_2 = \mathcal{O}(m_t). \quad (3.4)$$

The external momenta p_i and the Mandelstam invariants are obviously small, i.e. of $\mathcal{O}(1)$, in both regions. The expansion of any loop integral is a sum over the two regions. The contribution of each region is obtained by expanding the integrand for $m_t \rightarrow \infty$ assuming the loop momenta scale as in (3.3) for the large region and (3.4) for the small region.

The expansions in the large region, defined by (3.3), yields vacuum integrals of the form

$$\int d^{4-2\epsilon} k_1 d^{4-2\epsilon} k_2 \frac{1}{(k_1^2)^{a_1} (k_2^2 - m_t^2)^{a_2} ((k_1 + k_2)^2 - m_t^2)^{a_3}} \quad (3.5)$$

which can all be reduced to products of two one-loop tadpole integrals with mass m_t . In order to map the Laurent expansions of the integrands to integrals belonging to the family defined in (3.5), we first need to remove scalar products of the form $k_i \cdot p_j$ from the numerators of the expansions. This is done via a Passarino-Veltman decomposition [39], which in this case is very simple since it only depends on the metric tensor $g_{\mu\nu}$ (it can equivalently be performed via an angular integration, see e.g. [40]).

The expansion in the small region, defined by (3.4), yields instead products of one-loop tadpole integrals with mass m_t , times four-point one-loop integrals with massless internal propagators, i.e. belonging to the following family

$$\int d^{4-2\epsilon} k_2 \frac{1}{(k_2^2 - m_t^2)^{a_1}} \times \int d^{4-2\epsilon} k_1 \frac{1}{(k_1^2)^{2a_2} (k_1 + p_1)^{2a_3} (k_1 + p_{12})^{2a_4} (k_1 + p_{123})^{2a_5}} \quad (3.6)$$

with $p_{i_1 i_2 \dots} \equiv p_{i_1} + p_{i_2} + \dots$, or to families obtained from (3.6) via permutations of external momenta. The one-loop integrals in k_1 are the same integrals that contribute to the one-loop amplitude for diagrams without massive fermions. Similarly as before, we remove scalar products of the form $k_2 \cdot p_j$ and $k_1 \cdot k_2$ from the numerators of the expansion via a simple Passarino-Veltman decomposition for the one-loop integral in k_1 , where only the metric tensor $g_{\mu\nu}$ appears.

We also have a set of diagrams with two massive fermion loops. These can be cast as products of two one-loop integrals and only contribute to the large region in (3.3), where k_1 and k_2 are the two loop momenta. After expanding the integrands, these diagrams yield products of two massive one-loop tadpole integrals, which can also be mapped to the family in (3.5).

As a check of the consistency of the procedure, we used FINITEFLOW [41, 42] to verify, for a selection of integrals, that the expansion by regions commutes with the reduction to master integrals. In other words, we reconstructed the full m_t dependence of the reduction for a selection of two-loop integrals contributing to the process. We thus performed an expansion by regions of the left-hand sides and the right-hand sides of the reduction identities, verifying that they agree after a further reduction to the master integrals of the families in (3.5) and (3.6).

After reduction to master integrals, the expansion can be expressed in terms of (products of) simple one-loop master integrals, namely one-loop massive tadpole integrals and the

massless integrals appearing in the one-loop amplitude. In particular, all contributions to the pure-singlet axial amplitudes up to $\mathcal{O}(1/m_t^2)$ can be expressed in terms of massless one-loop two-point integrals and one-loop massive tadpoles.

3.2.1 The unrenormalised form factors up to two loops

Putting everything together, we obtain a result for the unrenormalised form factors, including the non-singlet and pure-singlet corrections up to two loops both for the vector and axial-vector couplings in massless QCD. Moreover, we also compute the axial-vector pure-singlet corrections for massive internal top quarks, keeping the m_t^0 and $1/m_t^2$ terms in an expansion in inverse powers in m_t . While ultimately being interested only in the exact $m_t \rightarrow \infty$ limit, keeping the next term in the expansion as intermediate step allows us to perform non-trivial checks on our approach.

We write for the unrenormalised form factors

$$\begin{aligned}\bar{F}_i &= \bar{F}_i^{(0)} + \left(\frac{\bar{\alpha}_s}{2\pi}\right) \bar{F}_i^{(1)} + \left(\frac{\bar{\alpha}_s}{2\pi}\right)^2 \bar{F}_i^{(2)} + \mathcal{O}(\bar{\alpha}_s^3) \\ \bar{G}_i &= \bar{G}_i^{(0)} + \left(\frac{\bar{\alpha}_s}{2\pi}\right) \bar{G}_i^{(1)} + \left(\frac{\bar{\alpha}_s}{2\pi}\right)^2 \bar{G}_i^{(2)} + \mathcal{O}(\bar{\alpha}_s^3),\end{aligned}\quad (3.7)$$

where $\bar{\alpha}_s$ is the bare strong coupling constant. We use consistently barred symbols for unrenormalised quantities.

The tree-level contributions to the form factors are not affected by renormalization, such that $F_i^{(0)} = \bar{F}_i^{(0)}$ and $G_i^{(0)} = \bar{G}_i^{(0)}$. The expressions for the tree-level form factors also allow us to elaborate upon the statement made in the context of (2.10) on the choice that we made for the tensor multiplying form factor G_6 . This choice turns out to be the only one of those described above that is entirely consistent with the 't Hooft-Veltman prescription. It is only with this choice that we find that the corresponding tree-level form factors to be exactly d -independent. We stress that this is a highly non-trivial finding, since all algebra at intermediate steps is performed in d dimensions, see (2.15). Explicitly, for the vector tree-level contribution we find

$$\begin{aligned}F_1^{(0)} &= 0, & F_2^{(0)} &= -\frac{2(s_{13} + s_{23})}{s_{12}s_{13}s_{23}}, & F_3^{(0)} &= \frac{s_{13} - s_{23}}{s_{13}s_{23}}, \\ F_4^{(0)} &= \frac{-s_{23}^2 - s_{12}s_{23} - s_{13}s_{23} + s_{12}s_{13}}{s_{12}s_{13}s_{23}}, & F_5^{(0)} &= \frac{s_{13}^2 + s_{12}s_{13} + s_{23}s_{13} - s_{12}s_{23}}{s_{12}s_{13}s_{23}}, \\ F_6^{(0)} &= \frac{2s_{12} + s_{13} + s_{23}}{s_{12}s_{13}}\end{aligned}\quad (3.8)$$

Similarly, for the axial-vector tree-level (which is only of non-singlet type) contribution we have

$$\begin{aligned}G_1^{(0)} &= -\frac{-s_{23}^2 - s_{12}s_{23} - 3s_{13}s_{23} + s_{12}s_{13}}{s_{12}s_{13}^2s_{23}^2}, & G_2^{(0)} &= -\frac{s_{13}^2 + s_{12}s_{13} + 3s_{23}s_{13} - s_{12}s_{23}}{s_{12}s_{13}^2s_{23}^2}, \\ G_3^{(0)} &= -\frac{4s_{12} + s_{13} + 3s_{23}}{s_{12}s_{13}^2s_{23}}, & G_4^{(0)} &= -\frac{2(2s_{12}^2 + s_{13}s_{12} + 3s_{23}s_{12} + s_{23}^2 - s_{13}s_{23})}{s_{12}^2s_{13}^2s_{23}}, \\ G_5^{(0)} &= -\frac{2(2s_{12}^2 + 3s_{13}s_{12} + s_{23}s_{12} + s_{13}^2 - s_{13}s_{23})}{s_{12}^2s_{13}^2s_{23}}, & G_6^{(0)} &= -\frac{s_{13} - s_{23}}{s_{12}s_{13}s_{23}}.\end{aligned}\quad (3.9)$$

All form factors receive non-singlet contributions, which we denote by $\bar{F}_i^{(0,1,2),n}$ and $\bar{G}_i^{(0,1,2),n}$. The pure-singlet contributions only enter at two loops in the vector form factors, denoted by $\bar{F}_i^{(2),p}$, due to a generalization of Furry's theorem [43], and at one and two loops in the axial-vector form factors, denoted by $\bar{G}_i^{(1,2),p}$. Since pure-singlet and non-singlet contributions will be dressed with different electroweak charge factors, they are treated separately throughout.

4 UV renormalisation and subtraction of the IR poles

The unrenormalised form factors (3.7) contain in general divergences both of ultraviolet (UV) and infrared (IR) origin, which manifest as poles in the dimensional regulator parameter ϵ .

UV poles can be consistently removed by the procedure of renormalisation. In our case, renormalisation proceeds differently in the purely vector and axial-vector cases and in the non-singlet and pure-singlet contributions, for two different reasons. First of all, as already discussed, due to the axial anomaly the pure-singlet axial-vector contribution can only be computed consistently in the full Standard Model if the closed quark loop is summed over a complete isospin doublet. A well-defined result for the pure-singlet axial-vector contribution with a single quark flavour in the loop requires an extra renormalization of the axial-vector pure-singlet current [28]. This pure-singlet renormalization of the axial anomaly is required for any γ_5 scheme. Secondly, since we work in the Larin scheme, the non-singlet axial-vector coupling also requires a renormalization to obtain consistent results [28].

We ultimately include top-quark effects in the exact $m_t \rightarrow \infty$ limit, but also compute corrections up to order $1/m_t^2$ in order to consistently check our renormalisation procedure. The formulae below reflect therefore the full renormalisation procedure required up to this order in $1/m_t$.

According to the discussion above, we renormalise α_s by replacing the bare coupling constant as follows

$$\bar{\alpha}_s \mu_0^{2\epsilon} S_\epsilon = \alpha_s \mu_R^{2\epsilon} \left[1 - \frac{1}{\epsilon} (\beta_0 + N_h \delta_w) \left(\frac{\alpha_s}{2\pi} \right) + \left(\frac{\beta_0^2}{\epsilon^2} - \frac{\beta_1}{2\epsilon} \right) \left(\frac{\alpha_s}{2\pi} \right)^2 + \mathcal{O}(\alpha_s^3) \right] \quad (4.1)$$

where $S_\epsilon = (4\pi)^\epsilon e^{-\epsilon\gamma_E}$, with $\gamma_E = 0.5772\dots$ the Euler-Mascheroni constant,

$$\delta_w = -\frac{2}{3} T_R \left(\frac{m_t^2}{\mu_R^2} \right)^{-\epsilon}. \quad (4.2)$$

We also introduced N_h for the number of heavy flavours of mass m_t , such that $N_h = 1$ for the pure-singlet axial-vector contribution and zero otherwise. We use the tag N_h to compactly include the dependence on the top mass in the beta function only for the pure-singlet axial-vector contribution, which in this calculation is required only to first order in α_s to renormalise the two-loop amplitude. β_i are the coefficients of the massless QCD beta function and read

$$\beta_0 = \frac{11}{6} C_A - \frac{4}{6} T_R N_f, \quad \beta_1 = \frac{17}{6} C_A^2 - \frac{10}{6} T_R C_A N_f - T_R C_F N_f, \quad (4.3)$$

where for $SU(N)$ we have

$$C_A = N, \quad C_F = \frac{N^2 - 1}{2N}, \quad T_R = \frac{1}{2},$$

with N the number of colors and N_f the number of active massless flavours. We must keep in mind that an overall factor of $\bar{\alpha}_s^{1/2}$ is contained in the relation (2.6) between amplitudes and form factors. For simplicity, we set $\mu_0^2 = \mu_R^2 = s_{12} + s_{13} + s_{23} = q^2$ throughout.

In addition to this, the renormalisation of the non-singlet axial-vector current requires multiplying the non-singlet contributions to the axial-vector form factors G_i by the non-singlet renormalisation constant, whose explicit value depends on the scheme used for treating γ_5 . In the Larin scheme, the latter is known up to four loops [44]. We only require its value up to two loops in our calculation:

$$Z_a^n = 1 - 2C_F \left(\frac{\alpha_s}{2\pi} \right) + \left[\frac{11}{2} C_F^2 - \frac{107}{36} C_F C_A + \frac{1}{18} C_F N_f \right] \left(\frac{\alpha_s}{2\pi} \right)^2 + \mathcal{O}(\alpha_s^3) \quad (4.4)$$

The renormalization of the axial-vector current is usually stated [28] in the form of renormalization constants for the non-singlet and the singlet currents, with the singlet current being the sum of non-singlet and pure-singlet. We choose instead to reformulate the renormalization in terms of non-singlet and pure-singlet, as introduced in [45]. In this form, the currents are mapped more easily onto the electroweak coupling factors, but at the expense of a mixing of non-singlet into pure-singlet contributions under renormalization. The pure-singlet renormalization constant starts only at order α_s^2 and reads [28] for a single quark flavour:

$$Z_a^s = C_F T_R \left(\frac{\alpha_s}{2\pi} \right)^2 \left[\frac{3}{2\epsilon} + \frac{3}{4} \right] + \mathcal{O}(\alpha_s^3), \quad (4.5)$$

where the pole part stems from the UV renormalization of the axial anomaly and the finite part is required to restore the axial Ward identities in dimensional regularization in the Larin scheme.

Finally, for what concerns the pure-singlet contributions from virtual top quarks to the axial-vector form factors, we also renormalise m_t in the on-shell scheme

$$\bar{m}_t = m_t \left[1 + \left(\frac{\alpha_s}{2\pi} \right) \delta_m \right] + \mathcal{O}(\alpha_s^2) \quad (4.6)$$

where \bar{m}_t is the bare mass and

$$\delta_m = C_F \left(\frac{m_t^2}{\mu_R^2} \right)^{-\epsilon} \left(-\frac{3}{2\epsilon} - 2 + \mathcal{O}(\epsilon) \right). \quad (4.7)$$

Finally, for these contributions gluon wave function renormalisation is performed by multiplying the pure-singlet axial-vector part of the form factors with

$$Z_A^{1/2} = 1 + \frac{1}{2} \left(\frac{\alpha_s}{2\pi} \right) N_h \delta_w + \mathcal{O}(\alpha_s^2) \quad (4.8)$$

since there is only one external gluon.

The UV-renormalized form factors are expanded in the renormalized coupling constant $\alpha_s = \alpha_s(\mu^2)$:

$$\begin{aligned} F_i &= F_i^{(0)} + \left(\frac{\alpha_s}{2\pi}\right) F_i^{(1)} + \left(\frac{\alpha_s}{2\pi}\right)^2 F_i^{(2)} + \mathcal{O}(\alpha_s^3), \\ G_i &= G_i^{(0)} + \left(\frac{\alpha_s}{2\pi}\right) G_i^{(1)} + \left(\frac{\alpha_s}{2\pi}\right)^2 G_i^{(2)} + \mathcal{O}(\alpha_s^3). \end{aligned} \quad (4.9)$$

We again distinguish non-singlet and pure-singlet contributions by a superscript (n, p) .

Putting everything together, we obtain renormalised form factors for the various contributions. For the vector form factors, we find for non-singlet and pure-singlet contributions:

$$\begin{aligned} F_i^{(0),n} &= \bar{F}_i^{(0),n}, \\ F_i^{(1),n} &= S_\epsilon^{-1} \bar{F}_i^{(1),n} - \frac{\beta_0}{2\epsilon} \bar{F}_i^{(0),n}, \\ F_i^{(2),n} &= S_\epsilon^{-2} \bar{F}_i^{(2),n} - \frac{3\beta_0}{2\epsilon} \bar{F}_i^{(1),n} S_\epsilon^{-1} - \left(\frac{\beta_1}{4\epsilon} - \frac{3\beta_0^2}{8\epsilon^2}\right) F_i^{(0),n}, \end{aligned} \quad (4.10)$$

$$F_i^{(2),p} = \bar{F}_i^{(2),p}, \quad (4.11)$$

while for the axial-vector non-singlet part we have

$$\begin{aligned} G_i^{(0),n} &= \bar{G}_i^{(0),n}, \\ G_i^{(1),n} &= S_\epsilon^{-1} \bar{G}_i^{(1),n} - \frac{\beta_0}{2\epsilon} \bar{G}_i^{(0),n} - 2C_F \bar{G}_i^{(0),n}, \\ G_i^{(2),n} &= S_\epsilon^{-2} \bar{G}_i^{(2),n} - \frac{3\beta_0}{2\epsilon} \bar{G}_i^{(1),n} S_\epsilon^{-1} - \left(\frac{\beta_1}{4\epsilon} - \frac{3\beta_0^2}{8\epsilon^2}\right) \bar{G}_i^{(0),n} \\ &\quad - 2C_F \bar{G}_i^{(1),n} S_\epsilon^{-1} + \left(\frac{2\beta_0}{\epsilon} + \frac{11}{2} C_F^2 - \frac{107}{36} C_F C_A + \frac{1}{18} C_F N_f\right) \bar{G}_i^{(0),n}, \end{aligned} \quad (4.12)$$

where we stress that the extra terms in comparison to (4.10) stem from the renormalisation of the axial-vector current in Larin's scheme.

For the pure-singlet axial-vector form factors, we consider the contributions from virtual massless and virtual massive quarks separately. We assemble the resulting one-loop and two-loop pure-singlet contributions to the form factors depending on whether the axial-vector current couples to a massless quark ($\bar{G}_i^{(j),p0}$) or to a massive quark ($\bar{G}_i^{(j),pm}$) of mass m_t . It should be noted that both these contributions contain massive and massless quark bubble insertions into their gluon propagators and external gluon legs.

With this in mind, the renormalization of the pure-singlet axial-vector form factors reads:

$$\begin{aligned} G_i^{(1),p0} &= S_\epsilon^{-1} \bar{G}_i^{(1),p0}, \\ G_i^{(1),pm} &= S_\epsilon^{-1} \bar{G}_i^{(1),pm}, \\ G_i^{(2),p0} &= S_\epsilon^{-2} \bar{G}_i^{(2),p0} - \left(\frac{3\beta_0}{2\epsilon} + \frac{N_h \delta_w}{\epsilon}\right) S_\epsilon^{-1} \bar{G}_i^{(1),p0} + C_F T_R \left(\frac{3}{2\epsilon} + \frac{3}{4}\right) \bar{G}_i^{(0),n}, \end{aligned}$$

$$\begin{aligned}
G_i^{(2),pm} &= S_\epsilon^{-2} \bar{G}_i^{(2),pm} - \left(\frac{3\beta_0}{2\epsilon} + \frac{N_h \delta_w}{\epsilon} \right) S_\epsilon^{-1} \bar{G}_i^{(1),pm} + S_\epsilon^{-1} \frac{d\bar{G}_i^{(1),pm}}{dm_t} \delta_m \\
&\quad + C_F T_R \left(\frac{3}{2\epsilon} + \frac{3}{4} \right) \bar{G}_i^{(0),n}, \tag{4.13}
\end{aligned}$$

where the last term on the right hand sides of the last two equations comes from the renormalization (4.5) of the axial anomaly. These terms cancel out in the difference $G_i^{(2),pm} - G_i^{(2),p0}$, since the summation over an isospin doublet renders the theory anomaly-free.

The renormalised form factors still have poles of IR nature. IR singularities in QCD are universal and their structure only depends on the number and type of strongly interacting partons involved in the scattering process [46–48]. For the case under study, we write the finite remainders in terms of the renormalised coefficients as:

$$\begin{aligned}
F_{i,\text{fin}}^{(1),n} &= F_i^{(1),n} - I_1(\epsilon) F_i^{(0),n}, \\
F_{i,\text{fin}}^{(2),n} &= F_i^{(2),n} - I_1(\epsilon) F_i^{(1),n} - I_2(\epsilon) F_i^{(0),n}, \\
G_{i,\text{fin}}^{(1),n} &= G_i^{(1),n} - I_1(\epsilon) G_i^{(0),n}, \\
G_{i,\text{fin}}^{(2),n} &= G_i^{(2),n} - I_1(\epsilon) G_i^{(1),n} - I_2(\epsilon) G_i^{(0),n}, \tag{4.14}
\end{aligned}$$

and

$$\begin{aligned}
G_{i,\text{fin}}^{(2),p0} &= G_i^{(2),p0} - I_1(\epsilon) G_i^{(1),p0}, \\
G_{i,\text{fin}}^{(2),pm} &= G_i^{(2),pm} - I_1(\epsilon) G_i^{(1),pm}. \tag{4.15}
\end{aligned}$$

We note that $F_i^{(2),p}$, $G_i^{(1),p0}$ and $G_i^{(1),pm}$ are already infrared-finite.

For our process, since we only have three coloured particles, the Catani operators [46] $I_1(\epsilon)$ and $I_2(\epsilon)$ are diagonal in color space. The operator I_1 reads

$$I_1(\epsilon) = -\frac{e^{\epsilon\gamma_E}}{2\Gamma(1-\epsilon)} \left[N \left(\frac{1}{\epsilon^2} + \frac{3}{4\epsilon} + \frac{\beta_0}{2N\epsilon} \right) (\mathbf{S}_{13} + \mathbf{S}_{23}) - \frac{1}{N} \left(\frac{1}{\epsilon^2} + \frac{3}{2\epsilon} \right) \mathbf{S}_{12} \right], \tag{4.16}$$

with

$$\mathbf{S}_{ij} = \left(-\frac{s_{ij}}{q^2} \right)^{-\epsilon}. \tag{4.17}$$

The operator $I_2(\epsilon)$ instead reads

$$I_2(\epsilon) = \frac{1}{2} I_1(\epsilon)^2 + \frac{\beta_0}{\epsilon} I_1(\epsilon) - e^{-\epsilon\gamma_E} \frac{\Gamma(1-2\epsilon)}{\Gamma(1-\epsilon)} \left(\frac{\beta_0}{\epsilon} + K \right) I_1(2\epsilon) - H_2(\epsilon), \tag{4.18}$$

where

$$H_2(\epsilon) = \frac{e^{\epsilon\gamma_E}}{4\epsilon\Gamma(2-\epsilon)} \mathbf{H}_2, \tag{4.19}$$

with

$$\begin{aligned}
\mathbf{H}_2 &= \left(4\zeta_3 + \frac{589}{432} - \frac{11\pi^2}{72} \right) N^2 + \left(-\frac{1}{2}\zeta_3 - \frac{41}{54} - \frac{\pi^2}{48} \right) + \left(-3\zeta_3 - \frac{3}{16} + \frac{\pi^2}{4} \right) \frac{1}{N^2} \\
&\quad + \left(-\frac{19}{18} + \frac{\pi^2}{36} \right) N N_f + \left(-\frac{1}{54} - \frac{\pi^2}{24} \right) \frac{N_f}{N} + \frac{5}{27} N_f^2, \tag{4.20}
\end{aligned}$$

and finally the constant K is

$$K = \left(\frac{67}{18} - \frac{\pi^2}{6} \right) C_A - \frac{10}{9} T_R N_f. \quad (4.21)$$

In all the above expressions for the Catani operators, N_f is taken equal to the number of light quark flavours in all non-singlet contributions, and equal to the number of light quark flavours plus one in the pure-singlet contributions.

The finiteness of (4.14) was already established [6] for the vector form factors. The finiteness of the axial-vector form factors, especially in the pure-singlet case (4.15), where it was also checked at order $1/m_t^2$ in the large-mass expansion, and which takes place prior to summation over an isospin doublet, represents a strong check on the internal consistency of our calculation.

5 The helicity amplitudes

The form factors that were computed in the previous section describe the coupling of an external off-shell vector or axial-vector current to a $q\bar{q}g$ -system. From these form factors, it is possible to reconstruct the helicity amplitudes for the decay of any vector boson $V = \gamma^*, Z, W^\pm$ into $q\bar{q}g$ by multiplying them by the appropriate electroweak couplings. Helicity amplitudes for vector-boson-plus-parton production can then be obtained by analytical continuation to the appropriately crossed kinematical regions [12].

5.1 Helicity amplitudes for an external vector and axial-vector current

It is useful to start off by considering the helicity amplitudes for the case of a generic vector or axial-vector current. We use the spinor helicity formalism and let the off-shell current decay to two massless leptons

$$V(p_4) \rightarrow l(p_5) + \bar{l}(p_6). \quad (5.1)$$

We call λ_f the helicity of fermion f and λ_3 the helicity of the external gluon $g(p_3)$. We define the left- and right-handed currents for a pair of fermions as

$$C_L^\mu(p, q) = \bar{u}_L(q)\gamma^\mu u_L(p) = \langle q\gamma^\mu p \rangle, \quad C_R^\mu(p, q) = \bar{u}_R(q)\gamma^\mu u_R(p) = [q\gamma^\mu p]. \quad (5.2)$$

The polarization vector for the external gluon, with positive and negative helicity respectively, is instead given by (remembering that we picked p_2 as gauge vector, and that the helicities are defined for p_3 outgoing)

$$\epsilon_{3,-}^\mu = \frac{\langle 3\gamma^\mu 2 \rangle}{\sqrt{2}\langle 32 \rangle}, \quad \epsilon_{3,+}^\mu = \frac{\langle 2\gamma^\mu 3 \rangle}{\sqrt{2}\langle 23 \rangle}. \quad (5.3)$$

Finally, in order to write down the helicity amplitudes starting from our general tensor structure in (2.9), we also use the following four-dimensional representation of the vector v_A^μ

$$v_A^\mu \equiv \epsilon^{p_1 p_2 p_3 \mu} = \frac{1}{4} \left[\langle 123\gamma^\mu 1 \rangle - \langle 123\gamma^\mu 1 \rangle \right]. \quad (5.4)$$

Note that, at this stage, v_A will only be contracted with four-dimensional external states, hence its four-dimensional representation is sufficient here, although d -dimensional identities were used in computing the form factors.

With these definitions, we consider the quantity

$$M_{\lambda_{q_2}\lambda_3\lambda_{l_5}} = \epsilon_{3,\rho}^{\lambda_3} A_{\lambda_{\bar{q}_1}\lambda_{q_2}}^{\mu\rho} C_{\lambda_{l_5}}^\mu(p_5, p_6), \quad (5.5)$$

where $A_{\lambda_{\bar{q}_1}\lambda_{q_2}}^{\mu\rho}$ is obtained from the general decomposition for the amplitude in (2.9) by fixing quark and gluon helicities. We stress that this means that we assign helicities according to the handedness of the outgoing fermions. We consider for definiteness the case of left-handed quark and lepton currents. By considering the vector and axial-vector current separately, we can write for both in spinor helicity formalism as

$$M_{L+L}^v = \frac{1}{\sqrt{2}} \left[\langle 12 \rangle [13]^2 (\alpha_1 \langle 536 \rangle + \alpha_2 \langle 526 \rangle) + \alpha_3 \langle 25 \rangle [13] [36] \right], \quad (5.6)$$

$$M_{L+L}^a = \frac{1}{\sqrt{2}} \left[\langle 12 \rangle [13]^2 (\beta_1 \langle 536 \rangle + \beta_2 \langle 526 \rangle) + \beta_3 \langle 25 \rangle [13] [36] \right], \quad (5.7)$$

where the superscript (v, a) indicate the vector and axial-vector parts. The coefficients α_i encompass the contribution from the former while the β_i indicate the latter. They can be written in terms of the original form factors as

$$\begin{aligned} \alpha_1 &= -F_1, & \alpha_2 &= F_2 - F_1 + \frac{2F_6}{s_{23}}, & \alpha_3 &= 2F_3 - \frac{2s_{12}F_6}{s_{23}}, \\ \beta_1 &= \frac{1}{2} \left[s_{23} (G_1 + G_3) + s_{12} (G_3 - G_4) \right], \\ \beta_2 &= \frac{1}{2} \left[s_{13}G_3 + s_{23} (G_1 - G_2 + G_3) - s_{12}G_4 + s_{12}G_5 - 2G_6 \right], \\ \beta_3 &= s_{12} (G_6 - s_{13}G_3). \end{aligned} \quad (5.8)$$

We stress that both the vector and the axial-vector part can be decomposed in terms of the same spinor structures.

Similarly, for the opposite choice of the gluon helicity we find

$$M_{L-L}^v = \frac{1}{\sqrt{2}} \left[\langle 23 \rangle^2 [12] (\gamma_1 \langle 536 \rangle + \gamma_2 \langle 516 \rangle) + \gamma_3 \langle 23 \rangle \langle 35 \rangle [16] \right], \quad (5.10)$$

$$M_{L-L}^a = \frac{1}{\sqrt{2}} \left[\langle 23 \rangle^2 [12] (\delta_1 \langle 536 \rangle + \delta_2 \langle 516 \rangle) + \delta_3 \langle 23 \rangle \langle 35 \rangle [16] \right], \quad (5.11)$$

where

$$\begin{aligned} \gamma_1 &= \frac{1}{s_{23}} \left[s_{13}F_2 + 2(F_5 - F_3) \right], \\ \gamma_2 &= \frac{1}{s_{23}} \left[s_{13}(F_2 - F_1) - 2(F_4 - F_5 + F_6) \right], \\ \gamma_3 &= -2 \frac{(s_{23}F_3 + s_{12}F_6)}{s_{23}}, \end{aligned} \quad (5.12)$$

$$\begin{aligned}
\delta_1 &= \frac{1}{2s_{23}} \left[s_{13}(s_{23}G_2 - (s_{12} + s_{13})G_3 + s_{12}G_5) - 2(s_{12} + s_{13})G_6 \right], \\
\delta_2 &= -\frac{1}{2s_{23}} \left[s_{13}^2 G_3 + 4s_{23}G_6 + s_{13}(s_{23}(G_1 - G_2 + G_3) + s_{12}G_4 - s_{12}G_5 + 2G_6) \right], \\
\delta_3 &= -s_{12}(s_{13}G_3 + 3G_6).
\end{aligned} \tag{5.13}$$

Similar relations can be written for a right-handed quark current, which are related to the ones above by parity conjugation, with a relative minus sign between vector and axial results,

$$M_{R+L}^v = -\frac{1}{\sqrt{2}} \left[[23]^2 \langle 12 \rangle (\gamma_1 \langle 536 \rangle + \gamma_2 \langle 516 \rangle) + \gamma_3 [23][36] \langle 15 \rangle \right], \tag{5.14}$$

$$M_{R+L}^a = \frac{1}{\sqrt{2}} \left[[23]^2 \langle 12 \rangle (\delta_1 \langle 536 \rangle + \delta_2 \langle 516 \rangle) + \delta_3 [23][36] \langle 15 \rangle \right], \tag{5.15}$$

$$M_{R-L}^v = -\frac{1}{\sqrt{2}} \left[[12] \langle 13 \rangle^2 (\alpha_1 \langle 536 \rangle + \alpha_2 \langle 526 \rangle) + \alpha_3 [26] \langle 13 \rangle \langle 35 \rangle \right], \tag{5.16}$$

$$M_{R-L}^a = \frac{1}{\sqrt{2}} \left[[12] \langle 13 \rangle^2 (\beta_1 \langle 536 \rangle + \beta_2 \langle 526 \rangle) + \beta_3 [26] \langle 13 \rangle \langle 35 \rangle \right], \tag{5.17}$$

where $\alpha_i, \beta_i, \gamma_i$ and δ_i are the same given above in terms of the form factors.

The finite remainder for vector and axial-vector helicity coefficients $\Omega_i = \{\alpha_i, \gamma_i\}$ and $\Lambda_i = \{\beta_i, \delta\}$ can be expanded as series in the strong coupling

$$\begin{aligned}
\Omega_i &= \Omega_i^{(0)} + \left(\frac{\alpha_s}{2\pi}\right) \Omega_i^{(1)} + \left(\frac{\alpha_s}{2\pi}\right)^2 \Omega_i^{(2)} + \mathcal{O}(\alpha_s^3), \\
\Lambda_i &= \Lambda_i^{(0)} + \left(\frac{\alpha_s}{2\pi}\right) \Lambda_i^{(1)} + \left(\frac{\alpha_s}{2\pi}\right)^2 \Lambda_i^{(2)} + \mathcal{O}(\alpha_s^3).
\end{aligned} \tag{5.18}$$

At l -loops, they inherit the corresponding decomposition into non-singlet and pure-singlet from the finite remainder of the form factors computed in the previous section. Moreover for the pure-singlet axial-vector case, we split them further into massless and massive contributions. We indicate the various components as above with $\Omega_i^{(l),n}, \Omega_i^{(l),p}, \Lambda_i^{(l),n}, \Lambda_i^{(l),p0}, \Lambda_i^{(l),pm}$ respectively.

At this point, we can perform an important consistency check on our calculation. We verified that after UV renormalisation and IR subtraction, as expected, the non-singlet contribution for the vector and axial-vector helicity amplitudes agree to the two-loop order. We find, in particular

$$\begin{aligned}
\alpha_i^{(0)} &= -\beta_i^{(0)} & \gamma_i^{(0)} &= -\delta_i^{(0)}, \\
\alpha_i^{(1),n} &= -\beta_i^{(1),n}, & \gamma_i^{(1),n} &= -\delta_i^{(1),n}, \\
\alpha_i^{(2),n} &= -\beta_i^{(2),n}, & \gamma_i^{(2),n} &= -\delta_i^{(2),n}.
\end{aligned} \tag{5.19}$$

The minus-sign between the α, γ (vector) and β, δ (axial-vector) coefficients arises from the definition of the basic vector and axial-vector amplitudes in terms of left-handed (V-A) quark

currents in (5.6), (5.7), which are then compensated by the explicit minus-signs between vector and axial-vector amplitudes for right-handed (V+A) quark currents in (5.14)–(5.17).

As exemplification of our results, we conclude this section by providing some analytic formulas for the axial-vector pure-singlet contributions. At tree level there is no pure-singlet contribution, so we provide the non-singlet results, which read

$$\beta_1^{(0)} = 0, \quad \beta_2^{(0)} = -\frac{4}{q^4} \frac{1}{yz}, \quad \beta_3^{(0)} = \frac{4}{q^2} \frac{1-y}{yz}, \quad (5.20)$$

$$\delta_1^{(0)} = 0, \quad \delta_2^{(0)} = \frac{4}{q^4} \frac{1}{yz}, \quad \delta_3^{(0)} = \frac{4}{q^2} \frac{1-z}{yz}. \quad (5.21)$$

At one loop instead we find for the pure-singlet contributions

$$\begin{aligned} \beta_1^{(1),pm} &= \beta_2^{(1),pm} = \beta_3^{(1),pm} = \mathcal{O}\left(\frac{1}{m_t^2}\right), \\ \delta_1^{(1),pm} &= \delta_2^{(1),pm} = \delta_3^{(1),pm} = \mathcal{O}\left(\frac{1}{m_t^2}\right), \end{aligned} \quad (5.22)$$

$$\beta_1^{(1),p0} = 0, \quad \beta_2^{(1),p0} = 0, \quad \beta_3^{(1),p0} = \frac{4}{q^2} \left[\frac{1}{y+z} + \frac{\log(1-y-z)}{(y+z)^2} \right], \quad (5.23)$$

$$\delta_1^{(1),p0} = 0, \quad \delta_2^{(1),p0} = 0, \quad \delta_3^{(1),p0} = \frac{4}{q^2} \left[\frac{1}{y+z} + \frac{\log(1-y-z)}{(y+z)^2} \right], \quad (5.24)$$

where we notice that, only at one-loop order, $\delta_i^{(1),p0} = \beta_i^{(1),p0}$ for $i = 1, 2, 3$.

Finally, at two loops the pure-singlet coefficients corresponding to the axial-vector current coupled to a massive quark loop are very compact. Limiting ourselves to the order zero in the large-mass expansion we find

$$\begin{aligned} \beta_1^{(2),pm} &= \mathcal{O}\left(\frac{1}{m_t^2}\right), \quad \beta_2^{(2),pm} = -\frac{3C_F}{q^4} \frac{1}{yz} \left[1 + 2 \log \frac{m_t^2}{q^2} \right] + \mathcal{O}\left(\frac{1}{m_t^2}\right), \\ \beta_3^{(2),pm} &= \frac{3C_F}{q^2} \frac{1-y}{yz} \left[1 + 2 \log \frac{m_t^2}{q^2} \right] + \mathcal{O}\left(\frac{1}{m_t^2}\right), \end{aligned} \quad (5.25)$$

$$\begin{aligned} \delta_1^{(2),pm} &= \mathcal{O}\left(\frac{1}{m_t^2}\right), \quad \delta_2^{(2),pm} = \frac{3C_F}{q^4} \frac{1}{yz} \left[1 + 2 \log \frac{m_t^2}{q^2} \right] + \mathcal{O}\left(\frac{1}{m_t^2}\right), \\ \delta_3^{(2),pm} &= \frac{3C_F}{q^2} \frac{1-z}{yz} \left[1 + 2 \log \frac{m_t^2}{q^2} \right] + \mathcal{O}\left(\frac{1}{m_t^2}\right). \end{aligned} \quad (5.26)$$

The corresponding results for the coupling to a massless quark loop are lengthier and can be obtained from the supplementary material attached to this paper in electronic format. As an example, we provide here the result for the $\beta_1^{(2),p0}$. We decompose it according to different powers of N as follows

$$\beta_1^{(2),p0} = \frac{1}{q^4} \left[NK_1 + \frac{1}{N} K_2 \right], \quad (5.27)$$

where the functions K_1 and K_2 are linear combinations of 2-dimensional harmonic polylogarithms with rational coefficients. In particular we find for the first

$$K_1 = \sum_{i=1}^{13} R_i Q_i,$$

with

$$\begin{aligned} R_1 &= \frac{1}{y^3}, & R_2 &= \frac{1}{y(z-1)}, & R_3 &= \frac{z}{(z-1)(y+z-1)^2}, & R_4 &= \frac{z}{y^2(y+z)^2}, \\ R_5 &= \frac{y-z+2}{y(z-1)(y+z)}, & R_6 &= \frac{3y+2z}{y^2(y+z)^2}, & R_7 &= \frac{5y^2+5yz+4z-4}{y(z-1)(y+z-1)(y+z)}, \\ R_8 &= \frac{y^2+6yz+3z^2}{y^2z(y+z)^2}, & R_9 &= \frac{5y^2-2yz+2y+4z^2-8z+4}{y^2(z-1)^3}, \\ R_{10} &= \frac{10y^3-y^2z^2+13y^2z-12y^2-6yz^2+12yz-6y-8z^3+24z^2-24z+8}{y^2(z-1)^2(y+z-1)^2}, \\ R_{11} &= \frac{2y^2+3yz^2-3yz+2y+3z^3-9z^2+10z-4}{y(z-1)^2(y+z-1)(y+z)}, \\ R_{12} &= \frac{y^2z+4yz^2-6yz+4y+3z^3-4z^2+2z}{y^2(z-1)(y+z)^2}, \\ R_{13} &= \frac{5y^3z+5y^3+8y^2z^2+10y^2z+2y^2+3yz^3-5yz^2+18yz-6y-8z^3+12z^2-4z}{y(z-1)^2z(y+z)^2}, \end{aligned}$$

and

$$\begin{aligned} Q_1 &= -12\zeta(3)G(1-z, y) - \frac{2}{3}\pi^2G(1, z)G(1-z, y) - 4G(0, 0, 1, z)G(1-z, y) \\ &\quad - 4G(1, 0, 1, z)G(1-z, y) + 4G(0, 1, z)G(1-z, 0, y) + \frac{2}{3}\pi^2G(1-z, 0, y) \\ &\quad - 4G(0, 1, z)G(1-z, 1-z, y) - \frac{2}{3}\pi^2G(1-z, 1-z, y) - 4G(1, 1, z)G(-z, 0, y) \\ &\quad + 4G(0, 1, z)G(-z, 1-z, y) + 4G(0, 1, z)G(-z, -z, y) + 4G(1, 1, z)G(-z, -z, y) \\ &\quad + 4G(0, 1, 1, z)G(-z, y) + 4G(1, 0, 1, z)G(-z, y) + 4G(1, z) \left[G(1-z, 0, -z, y) \right. \\ &\quad \left. - G(1-z, 1-z, -z, y) - G(-z, 0, 1-z, y) - G(-z, 1-z, 0, y) \right. \\ &\quad \left. + G(-z, 1-z, -z, y) - G(-z, -z, 0, y) + G(-z, -z, 1-z, y) + G(-z, -z, -z, y) \right] \\ &\quad - 4G(1-z, 0, 1, 0, y) + 4G(1-z, 0, -z, 1-z, y) + 4G(1-z, 1-z, 1, 0, y) \\ &\quad - 4G(1-z, 1-z, -z, 1-z, y) + 4G(-z, 0, 1, 0, y) - 4G(-z, 0, 1-z, 1-z, y) \\ &\quad - 4G(-z, 1-z, 0, 1-z, y) + 4G(-z, 1-z, 1, 0, y) - 4G(-z, 1-z, 1-z, 0, y) \\ &\quad + 4G(-z, 1-z, -z, 1-z, y) - 4G(-z, -z, 0, 1-z, y) - 4G(-z, -z, 1-z, 0, y) \\ &\quad + 4G(-z, -z, 1-z, 1-z, y) + 4G(-z, -z, -z, 1-z, y), \\ Q_2 &= \frac{1}{2}G(1-z, y) + \frac{1}{2}G(1, z) - 1, \\ Q_3 &= \frac{1}{2}G(0, y)G(0, z) - \frac{1}{2}G(1, z)G(-z, y) - \frac{1}{2}G(-z, 1-z, y) \\ &\quad - \frac{1}{2}G(0, 1, z) - \frac{1}{2}G(1, 0, z), \end{aligned}$$

$$\begin{aligned}
Q_4 = & G(1, z)G(0, 1 - z, y) - G(1, z)G(0, -z, y) + G(1, z)G(1 - z, 0, y) \\
& + G(1, z)G(-z, 0, y) - \frac{8}{3}G(1 - z, y) - G(0, 1, z)G(1 - z, y) - G(0, 1, z)G(-z, y) \\
& + G(0, z)G(0, 1 - z, y) - G(1, 0, z)G(-z, y) + G(0, y)G(1, 1, z) \\
& - G(0, z)G(1 - z, 1 - z, y) - G(0, z)G(-z, 1 - z, y) + G(0, 1 - z, 1 - z, y) \\
& - G(0, -z, 1 - z, y) + G(1 - z, 0, 1 - z, y) - G(1 - z, 1, 0, y) + G(1 - z, 1 - z, 0, y) \\
& + G(-z, 0, 1 - z, y) + G(-z, 1 - z, 0, y) + \frac{2}{3}G(1, 0, y) - G(0, 1, 0, y) - \frac{8}{3}G(1, z) \\
& - \frac{2}{3}G(1, 0, z) - G(0, 1, 1, z) - G(1, 0, 1, z),
\end{aligned}$$

$$Q_5 = 2G(1 - z, y) + 2G(1, z),$$

$$\begin{aligned}
Q_6 = & -2G(1, z)G(1 - z, y) + \frac{4}{3}G(1 - z, y) - 2G(1 - z, 1 - z, y) + \frac{5}{3}G(1, 0, y) \\
& + \frac{4}{3}G(1, z) + \frac{1}{3}G(1, 0, z) - 2G(1, 1, z),
\end{aligned}$$

$$Q_7 = -\frac{1}{2}G(0, y),$$

$$\begin{aligned}
Q_8 = & G(0, 1, z)(-G(1 - z, y)) - G(0, 1, z)G(-z, y) + G(1, z)G(0, 1 - z, y) \\
& + G(0, y)G(1, 1, z) - G(1, 1, z)G(-z, y) + G(1, z)G(1 - z, 0, y) \\
& - G(1, z)G(1 - z, -z, y) + G(1, z)G(-z, 0, y) - G(1, z)G(-z, 1 - z, y) \\
& - G(1, z)G(-z, -z, y) + G(0, 1 - z, 1 - z, y) + G(1 - z, 0, 1 - z, y) \\
& - G(1 - z, 1, 0, y) + G(1 - z, 1 - z, 0, y) - G(1 - z, -z, 1 - z, y) \\
& + G(-z, 0, 1 - z, y) + G(-z, 1 - z, 0, y) - G(-z, 1 - z, 1 - z, y) \\
& - G(-z, -z, 1 - z, y) - G(0, 1, 0, y) - G(0, 1, 1, z) - G(1, 0, 1, z),
\end{aligned}$$

$$\begin{aligned}
Q_9 = & G(0, y)(-G(0, 1, z)) + \frac{1}{6}\pi^2 G(1 - z, y) + G(0, 1, z)G(1 - z, y) \\
& - G(1, z)G(0, -z, y) + G(1, z)G(1 - z, -z, y) - G(0, -z, 1 - z, y) \\
& - G(1 - z, 1, 0, y) + G(1 - z, -z, 1 - z, y) - \frac{1}{6}\pi^2 [G(0, y) - G(1, z)] \\
& + G(0, 1, 0, y) + G(0, 0, 1, z) + G(1, 0, 1, z) + 3\zeta(3),
\end{aligned}$$

$$Q_{10} = -\frac{1}{2}G(1, z)G(-z, y) - \frac{1}{2}G(-z, 1 - z, y) + \frac{1}{2}G(1, 0, y) - \frac{1}{2}G(0, 1, z) - \frac{\pi^2}{12},$$

$$Q_{11} = \frac{1}{2}G(0, z),$$

$$Q_{12} = -\frac{1}{2}G(0, z)G(1 - z, y) + \frac{1}{2}G(1, z)G(-z, y) + \frac{1}{2}G(-z, 1 - z, y),$$

$$\begin{aligned}
Q_{13} = & \frac{1}{2}G(0, y)G(1, z) - \frac{1}{2}G(1, z)G(-z, y) + \frac{1}{2}G(0, 1 - z, y) + \frac{1}{2}G(1 - z, 0, y) \\
& - \frac{1}{2}G(-z, 1 - z, y) - \frac{1}{2}G(1, 0, y) - \frac{1}{2}G(0, 1, z).
\end{aligned}$$

For K_2 we write instead

$$K_2 = \sum_{i=14}^{19} R_i Q_i$$

with

$$\begin{aligned}
 R_{14} &= \frac{y-z+2}{y(z-1)(y+z)}, & R_{15} &= \frac{2z-y}{(y+z)^4}, & R_{16} &= \frac{2y+2z-3}{(y+z-1)(y+z)^2}, \\
 R_{17} &= \frac{(y-1)(y^3+y^2z-7y^2-yz^2-5yz+5y-z^3+2z^2-z)}{y(y+z-1)^2(y+z)^3}, \\
 R_{18} &= \frac{y^3+y^2z-3y^2-yz^2+3yz+2y-z^3+6z^2-4z}{(y+z-1)^2(y+z)^3}, \\
 R_{19} &= \frac{y^3+4y^2z^2-5y^2z+3y^2+4yz^3-9yz^2+10yz-4y+3z^3-5z^2+2z}{y(z-1)^2(y+z-1)(y+z)^2},
 \end{aligned}$$

and

$$\begin{aligned}
 Q_{14} &= 1, \\
 Q_{15} &= -\frac{2}{3}\pi^2 G(1-z, y) - 4G(0, y)G(1, 0, z) + 4G(1, 0, z)G(1-z, y) \\
 &\quad - 4G(0, z)G(1-z, 0, y) + 4G(1-z, 1, 0, y) + 4G(0, 1, 0, y) - \frac{2}{3}\pi^2 G(1, z) \\
 &\quad + 4G(0, 1, 0, z) + 4G(1, 1, 0, z), \\
 Q_{16} &= 2G(0, y), \\
 Q_{17} &= 2G(1, 0, z) - 2G(1, 0, y), \\
 Q_{18} &= 2G(0, y)G(0, z) - 4G(1, 0, z) + \frac{\pi^2}{3}, \\
 Q_{19} &= -G(0, z).
 \end{aligned}$$

As discussed above, the analytic results for the remaining coefficients can be found in the supplementary attached to this paper.

5.2 Helicity amplitudes for a Standard Model vector boson

We are now ready to build the helicity amplitudes for a standard model vector boson V connecting a $q\bar{q}g$ system and to a lepton-antilepton pair. We write the coupling of the vector boson V to two fermions $f_1 f_2$ in the two equivalent ways

$$\begin{aligned}
 -ie \Gamma_\mu^V f_1 f_2 &= -i\sqrt{4\pi\alpha} \left[v_{f_1 f_2}^V \gamma^\mu + a_{f_1 f_2}^V \gamma^\mu \gamma_5 \right] \\
 &= -i\sqrt{4\pi\alpha} \left[L_{f_1 f_2}^V \gamma^\mu \left(\frac{1-\gamma_5}{2} \right) + R_{f_1 f_2}^V \gamma^\mu \left(\frac{1+\gamma_5}{2} \right) \right]
 \end{aligned} \tag{5.28}$$

where clearly

$$L_{f_1 f_2}^V = v_{f_1 f_2}^V - a_{f_1 f_2}^V, \quad R_{f_1 f_2}^V = v_{f_1 f_2}^V + a_{f_1 f_2}^V$$

and for the three types of vector bosons we have

$$L_{f_1 f_2}^\gamma = R_{f_1 f_2}^\gamma = -e_{f_1} \delta_{f_1 f_2} \tag{5.29}$$

$$L_{f_1 f_2}^Z = \frac{I_3^{f_1} - \sin^2 \theta_w e_{f_1}}{\sin \theta_w \cos \theta_w} \delta_{f_1 f_2}, \quad R_{f_1 f_2}^Z = -\frac{\sin \theta_w e_{f_1}}{\cos \theta_w} \delta_{f_1 f_2} \tag{5.30}$$

$$L_{f_1 f_2}^W = \frac{\epsilon_{f_1, f_2}}{\sqrt{2} \sin \theta_w}, \quad R_{f_1 f_2}^W = 0. \tag{5.31}$$

In the formulas above α is the electroweak coupling constant, θ_w is the Weinberg angle, $I_3 = \pm 1/2$ is the third component of the weak isospin and in all formulas the charges e_i are measured in terms of the fundamental electric charge $e > 0$. Moreover, $\epsilon_{f_1, f_2} = 1$ if $f_1 \neq f_2$ but belonging to the same isospin doublet and zero otherwise. Finally, we write the propagator of the vector boson V of momentum q and mass m_V as $P_{\mu\nu}(q, m_V)$, whose expression in Lorentz gauge reads

$$P_{\mu\nu}(q, m_V) = \frac{i \left(-g_{\mu\nu} + \frac{q_\mu q_\nu}{q^2} \right)}{D(q^2, m_V^2)}, \quad (5.32)$$

with

$$D(q^2, m_V^2) = q^2 - m_V^2 + i\Gamma_V m_V.$$

From (5.28), we can immediately read off the coupling factors of all non-singlet contributions: $v_{f_1 f_2}^V$ for the vector form factors and $a_{f_1 f_2}^V$ for the axial-vector form factors. Consequently, when re-casting the form factors into helicity amplitudes, we expect each amplitude for a specific quark helicity to contain a linear combination of vector and axial-vector form factors.

In the pure-singlet contributions, the vertex (5.28) is coupled to an internal quark loop, thus requiring a summation over the internal quark flavours. In the vector case, this summation amounts to an overall factor

$$N_{f,\gamma}^v = \sum_q e_q, \quad N_{f,Z}^v = \sum_q \frac{(L_{qq}^Z + R_{qq}^Z)}{2}, \quad N_{f,W}^v = 0, \quad (5.33)$$

with the sums running over the active quark flavours. In the axial-vector case, the summation must be performed over complete quark isospin doublets. For mass-degenerate quarks in the doublet, the summation of up-type and down-type contribution cancels identically. In case of a mass-splitting in the doublet, the axial-vector pure-singlet contribution is obtained as the difference between up-type and down-type quark contributions in the loop, multiplied by a coupling factor

$$N_{f,\gamma}^a = 0, \quad N_{f,Z}^a = \frac{1}{4 \sin \theta_w \cos \theta_w}, \quad N_{f,W}^a = 0. \quad (5.34)$$

The last identity in (5.33) is a consequence of charge conservation while, as already discussed, there can be a contribution from the axial-vector coupling to the pure-singlet amplitude only in the case of the production of a Z boson.

With these definitions, we write the helicity amplitudes for a vector boson V as

$$\mathcal{M}_{L+L}^V = -\frac{i\sqrt{4\pi\alpha_s}(4\pi\alpha) L_{l_5 l_6}^V}{\sqrt{2} D(p_{56}^2, m_V^2)} \mathbb{T}_{ij}^a \left[\langle 12 \rangle [13]^2 (A_1 \langle 536 \rangle + A_2 \langle 526 \rangle) + A_3 \langle 25 \rangle [13] [36] \right], \quad (5.35)$$

$$\mathcal{M}_{L-L}^V = -\frac{i\sqrt{4\pi\alpha_s}(4\pi\alpha) L_{l_5 l_6}^V}{\sqrt{2} D(p_{56}^2, m_V^2)} \mathbb{T}_{ij}^a \left[\langle 23 \rangle^2 [12] (B_1 \langle 536 \rangle + B_2 \langle 516 \rangle) + B_3 \langle 23 \rangle \langle 35 \rangle [16] \right], \quad (5.36)$$

where $p_{56} = p_5 + p_6$. The l -loop coefficients can be written in terms of the l -loop Ω_i and Λ_i introduced above¹ as follows

$$A_i^{(l)} = L_{q_1 q_2}^V \alpha_i^{(l),n} + N_{f,V}^v \alpha_i^{(l),p} + N_{f,V}^a \left(\beta_i^{(l),p0} - \beta_i^{(l),pm} \right), \quad (5.37)$$

$$B_i^{(l)} = L_{q_1 q_2}^V \gamma_i^{(l),n} + N_{f,V}^v \gamma_i^{(l),p} + N_{f,V}^a \left(\delta_i^{(l),p0} - \delta_i^{(l),pm} \right), \quad (5.38)$$

where we used the fact that the non-singlet vector and axial-vector parts are equal after UV renormalisation and IR subtraction.

In the same way, we obtain for right-handed quarks

$$\mathcal{M}_{R+L}^V = \frac{i\sqrt{4\pi\alpha_s}(4\pi\alpha) L_{l_5 l_6}^V}{\sqrt{2} D(p_{56}^2, m_V^2)} \mathbb{T}_{ij}^a \left[[23]^2 \langle 12 \rangle \left(C_1 \langle 536 \rangle + C_2 \langle 516 \rangle \right) + C_3 [23] [36] \langle 15 \rangle \right], \quad (5.39)$$

$$\mathcal{M}_{R-L}^V = \frac{i\sqrt{4\pi\alpha_s}(4\pi\alpha) L_{l_5 l_6}^V}{\sqrt{2} D(p_{56}^2, m_V^2)} \mathbb{T}_{ij}^a \left[[12] \langle 13 \rangle^2 \left(D_1 \langle 536 \rangle + D_2 \langle 526 \rangle \right) + D_3 [26] \langle 13 \rangle \langle 35 \rangle \right], \quad (5.40)$$

with

$$C_i^{(l)} = R_{q_1 q_2}^V \gamma_i^{(l),n} + N_{f,V}^v \gamma_i^{(l),p} - N_{f,V}^a \left(\delta_i^{(l),p0} - \delta_i^{(l),pm} \right), \quad (5.41)$$

$$D_i^{(l)} = R_{q_1 q_2}^V \alpha_i^{(l),n} + N_{f,V}^v \alpha_i^{(l),p} - N_{f,V}^a \left(\beta_i^{(l),p0} - \beta_i^{(l),pm} \right). \quad (5.42)$$

We stress that the remaining four helicity amplitudes can be obtained from the ones given above, by a CP transformation *and changing all relevant couplings*. The CP transformation acts on the spinor products by swapping angle and square brackets, but it leaves the functional part of the coefficients unchanged.

5.3 Checks on the results

In deriving the results for the renormalized form factors in section 4 and the resulting helicity amplitudes in this section, we have performed various checks, which we briefly summarize in the following.

The infrared pole structure of the form factors at one loop and two loops can be predicted in terms of universal IR pole operators and lower-order results, as described in (4.14), (4.15). We observe that all form factors up to two loops reproduce the predicted IR pole structure. This is a particularly strong check for what concerns the axial-vector part of the result, since the latter requires non-trivial UV renormalisation, which depends on the scheme used to deal with γ_5 in dimensional regularisation.

As a second non-trivial check for our correct implementation of the Larin scheme, we have verified explicitly up to two loops that the non-singlet axial-vector and purely vector helicity amplitudes agree after UV renormalisation and IR subtraction, see (5.19).

The vector parts of the helicity amplitudes were computed previously up to two loops [6], and we reproduced these earlier results. The axial-vector singlet parts were only known to one-loop, and we verified that the resulting one-loop helicity amplitudes agree with the literature [21].

¹See discussion around (5.18).

Finally, we performed a thorough check of the helicity amplitudes up to one loop against OPENLOOPS2 [49, 50], both for the exchange of a virtual photon and of a Z boson. This allowed us to validate all electroweak couplings, including the overall normalisation of $N_{f,Z}^a$, see (5.34).

6 Conclusions

The two-loop helicity amplitudes for $V \rightarrow q\bar{q}g$ constitute the purely virtual contribution to the NNLO corrections to $e^+e^- \rightarrow 3$ jets, as well as in different kinematical crossings to $ep \rightarrow (2+1)$ jets and $pp \rightarrow V+1$ jet. They were computed already long ago [5, 6] for a purely vector-like coupling of the boson V . Owing to chirality conservation for massless fermions, these results can be extended in a straightforward manner to an axial-vector coupling of V [6, 31] for non-singlet type contributions, where the vector boson couples to the external quark line. These amplitudes were used subsequently in the NNLO calculations for the above processes in e^+e^- annihilation [7, 9, 10], deeply inelastic electron-proton collisions [51] and proton-proton collisions [16–18].

In this paper, we complete the computation of the two-loop $V \rightarrow q\bar{q}g$ helicity amplitudes by deriving the previously missing pure-singlet axial-vector contributions. Our calculation is enabled by the construction of a new four-dimensional tensor basis [25, 26] for the $V \rightarrow q\bar{q}g$ amplitudes, which avoids the introduction of evanescent tensor structures and allows a consistent application of the Larin scheme for axial couplings in dimensional regularization in the computation of the associated form factors. In this new basis, we rederive the non-singlet helicity amplitudes at two loops, confirming the earlier results [5, 6] and explicitly demonstrating the equivalence of vector and axial-vector amplitudes in the non-singlet case, after renormalization and IR factorization.

In the pure-singlet axial-vector amplitudes, the vector boson couples to an internal quark loop. These amplitudes are affected by the axial anomaly, which cancels in the electroweak Standard Model upon summation over weak isospin doublets. We compute the two-loop pure-singlet axial-vector form factors, separately for massless internal quarks and in a large-mass expansion for massive internal quarks, and recovering in both cases the correct universal divergent behaviour of the axial anomaly. Subleading terms in the large-mass expansion are also computed to demonstrate the internal consistency of the approach. The combination of massless and massive internal quarks describes the pure-singlet axial-vector contribution from top-bottom mass splitting.

By combining our newly derived two-loop pure-singlet axial-vector amplitudes with the other pure-singlet contributions that contribute at the same order [19–21], it will now be possible to consistently compute the axial-vector pure-singlet contributions to V +jet production at NNLO. Moreover, in combination with the recently derived three-loop pure-singlet axial-vector quark form factors [45, 52], these results can be extended to differential cross sections in Z boson production at N3LO.

Besides their potential relevance for differential lepton pair distributions in Z and Z +jet production processes at hadron colliders, the pure-singlet axial-vector contribution could also have an impact on three-jet production observables at e^+e^- colliders, especially on the event orientation [53] and on oriented event shapes derived from it.

Acknowledgments

We are grateful to Federico Buccioni for his assistance and patience in helping us check our results against OPENLOOPS2, and to Fabrizio Caola for useful comments on the manuscript. This work was supported in part by the Excellence Cluster ORIGINS funded by the Deutsche Forschungsgemeinschaft (DFG, German Research Foundation) under Germany's Excellence Strategy – EXC-2094-390783311, by the Swiss National Science Foundation (SNF) under contract 200020-204200, and by the European Research Council (ERC) under the European Union's research and innovation programme grant agreements 949279 (ERC Starting Grant HighPHun), 101040760 (ERC Starting Grant FFHiggsTop) and 101019620 (ERC Advanced Grant TOPUP).

Open Access. This article is distributed under the terms of the Creative Commons Attribution License ([CC-BY 4.0](https://creativecommons.org/licenses/by/4.0/)), which permits any use, distribution and reproduction in any medium, provided the original author(s) and source are credited. SCOAP³ supports the goals of the International Year of Basic Sciences for Sustainable Development.

References

- [1] D.P. Barber et al., *Discovery of Three Jet Events and a Test of Quantum Chromodynamics at PETRA Energies*, *Phys. Rev. Lett.* **43** (1979) 830 [[INSPIRE](#)].
- [2] J.R. Ellis, M.K. Gaillard and G.G. Ross, *Search for Gluons in e^+e^- Annihilation*, *Nucl. Phys. B* **111** (1976) 253 [[INSPIRE](#)].
- [3] R.K. Ellis, D.A. Ross and A.E. Terrano, *The Perturbative Calculation of Jet Structure in e^+e^- Annihilation*, *Nucl. Phys. B* **178** (1981) 421 [[INSPIRE](#)].
- [4] W.T. Giele and E.W.N. Glover, *Higher order corrections to jet cross-sections in e^+e^- annihilation*, *Phys. Rev. D* **46** (1992) 1980 [[INSPIRE](#)].
- [5] L.W. Garland, T. Gehrmann, E.W.N. Glover, A. Koukoutsakis and E. Remiddi, *The Two loop QCD matrix element for $e^+e^- \rightarrow 3$ jets*, *Nucl. Phys. B* **627** (2002) 107 [[hep-ph/0112081](#)] [[INSPIRE](#)].
- [6] L.W. Garland, T. Gehrmann, E.W.N. Glover, A. Koukoutsakis and E. Remiddi, *Two loop QCD helicity amplitudes for $e^+e^- \rightarrow 3$ jets*, *Nucl. Phys. B* **642** (2002) 227 [[hep-ph/0206067](#)] [[INSPIRE](#)].
- [7] A. Gehrmann-De Ridder, T. Gehrmann, E.W.N. Glover and G. Heinrich, *NNLO corrections to event shapes in e^+e^- annihilation*, *JHEP* **12** (2007) 094 [[arXiv:0711.4711](#)] [[INSPIRE](#)].
- [8] A. Gehrmann-De Ridder, T. Gehrmann, E.W.N. Glover and G. Heinrich, *Jet rates in electron-positron annihilation at $O(\alpha_s^3)$ in QCD*, *Phys. Rev. Lett.* **100** (2008) 172001 [[arXiv:0802.0813](#)] [[INSPIRE](#)].
- [9] S. Weinzierl, *Event shapes and jet rates in electron-positron annihilation at NNLO*, *JHEP* **06** (2009) 041 [[arXiv:0904.1077](#)] [[INSPIRE](#)].
- [10] V. Del Duca, C. Duhr, A. Kardos, G. Somogyi and Z. Trócsányi, *Three-Jet Production in Electron-Positron Collisions at Next-to-Next-to-Leading Order Accuracy*, *Phys. Rev. Lett.* **117** (2016) 152004 [[arXiv:1603.08927](#)] [[INSPIRE](#)].

- [11] D. Graudenz, *Next-to-leading order QCD corrections to jet cross-sections and jet rates in deeply inelastic electron proton scattering*, *Phys. Rev. D* **49** (1994) 3291 [[hep-ph/9307311](#)] [[INSPIRE](#)].
- [12] T. Gehrmann and E. Remiddi, *Analytic continuation of massless two loop four point functions*, *Nucl. Phys. B* **640** (2002) 379 [[hep-ph/0207020](#)] [[INSPIRE](#)].
- [13] D.A. Dicus and S.S.D. Willenbrock, *Radiative Corrections to the Ratio of Z and W Boson Production*, *Phys. Rev. D* **34** (1986) 148 [[INSPIRE](#)].
- [14] K. Hagiwara, T. Kuruma and Y. Yamada, *Three jet distributions from the one loop Zgg vertex at e^+e^- colliders*, *Nucl. Phys. B* **358** (1991) 80 [[INSPIRE](#)].
- [15] K. Hagiwara, T. Kuruma and Y. Yamada, *Probing the one loop Z g g vertex at hadron colliders*, *Nucl. Phys. B* **369** (1992) 171 [[INSPIRE](#)].
- [16] A. Gehrmann-De Ridder, T. Gehrmann, E.W.N. Glover, A. Huss and T.A. Morgan, *Precise QCD predictions for the production of a Z boson in association with a hadronic jet*, *Phys. Rev. Lett.* **117** (2016) 022001 [[arXiv:1507.02850](#)] [[INSPIRE](#)].
- [17] R. Boughezal et al., *Z-boson production in association with a jet at next-to-next-to-leading order in perturbative QCD*, *Phys. Rev. Lett.* **116** (2016) 152001 [[arXiv:1512.01291](#)] [[INSPIRE](#)].
- [18] T. Neumann and J. Campbell, *Fiducial Drell-Yan production at the LHC improved by transverse-momentum resummation at $N^4LL + N^3LO$* , FERMILAB-PUB-22-528-T (2022) [[arXiv:2207.07056](#)] [[INSPIRE](#)].
- [19] J.J. van der Bij and E.W.N. Glover, *Z Boson Production and Decay via Gluons*, *Nucl. Phys. B* **313** (1989) 237 [[INSPIRE](#)].
- [20] R. Höpker and J.J. van der Bij, *Z^0 decay into three gluons*, *Phys. Rev. D* **49** (1994) 3779 [[INSPIRE](#)].
- [21] Z. Bern, L.J. Dixon and D.A. Kosower, *One loop amplitudes for e^+e^- to four partons*, *Nucl. Phys. B* **513** (1998) 3 [[hep-ph/9708239](#)] [[INSPIRE](#)].
- [22] C. Duhr and B. Mistlberger, *Lepton-pair production at hadron colliders at N^3LO in QCD*, *JHEP* **03** (2022) 116 [[arXiv:2111.10379](#)] [[INSPIRE](#)].
- [23] T. Gehrmann and E. Remiddi, *Two loop master integrals for $\gamma^* \rightarrow 3$ jets: The Planar topologies*, *Nucl. Phys. B* **601** (2001) 248 [[hep-ph/0008287](#)] [[INSPIRE](#)].
- [24] T. Gehrmann and E. Remiddi, *Two loop master integrals for $\gamma^* \rightarrow 3$ jets: The Nonplanar topologies*, *Nucl. Phys. B* **601** (2001) 287 [[hep-ph/0101124](#)] [[INSPIRE](#)].
- [25] T. Peraro and L. Tancredi, *Physical projectors for multi-leg helicity amplitudes*, *JHEP* **07** (2019) 114 [[arXiv:1906.03298](#)] [[INSPIRE](#)].
- [26] T. Peraro and L. Tancredi, *Tensor decomposition for bosonic and fermionic scattering amplitudes*, *Phys. Rev. D* **103** (2021) 054042 [[arXiv:2012.00820](#)] [[INSPIRE](#)].
- [27] G. 't Hooft and M.J.G. Veltman, *Regularization and Renormalization of Gauge Fields*, *Nucl. Phys. B* **44** (1972) 189 [[INSPIRE](#)].
- [28] S.A. Larin, *The Renormalization of the axial anomaly in dimensional regularization*, *Phys. Lett. B* **303** (1993) 113 [[hep-ph/9302240](#)] [[INSPIRE](#)].
- [29] P. Nogueira, *Automatic Feynman graph generation*, *J. Comput. Phys.* **105** (1993) 279 [[INSPIRE](#)].

- [30] J.A.M. Vermaseren, *New features of FORM*, [math-ph/0010025](#) [INSPIRE].
- [31] T. Gehrmann and L. Tancredi, *Two-loop QCD helicity amplitudes for $q\bar{q} \rightarrow W^\pm\gamma$ and $q\bar{q} \rightarrow Z^0\gamma$* , *JHEP* **02** (2012) 004 [[arXiv:1112.1531](#)] [INSPIRE].
- [32] C. Studerus, *Reduze-Feynman Integral Reduction in C++*, *Comput. Phys. Commun.* **181** (2010) 1293 [[arXiv:0912.2546](#)] [INSPIRE].
- [33] A. von Manteuffel and C. Studerus, *Reduze 2 — Distributed Feynman Integral Reduction*, ZU-TH-01-12 (2012) [[arXiv:1201.4330](#)] [INSPIRE].
- [34] E. Remiddi and J.A.M. Vermaseren, *Harmonic polylogarithms*, *Int. J. Mod. Phys. A* **15** (2000) 725 [[hep-ph/9905237](#)] [INSPIRE].
- [35] T. Gehrmann and E. Remiddi, *Numerical evaluation of harmonic polylogarithms*, *Comput. Phys. Commun.* **141** (2001) 296 [[hep-ph/0107173](#)] [INSPIRE].
- [36] T. Gehrmann and E. Remiddi, *Numerical evaluation of two-dimensional harmonic polylogarithms*, *Comput. Phys. Commun.* **144** (2002) 200 [[hep-ph/0111255](#)] [INSPIRE].
- [37] J. Vollinga and S. Weinzierl, *Numerical evaluation of multiple polylogarithms*, *Comput. Phys. Commun.* **167** (2005) 177 [[hep-ph/0410259](#)] [INSPIRE].
- [38] M. Beneke and V.A. Smirnov, *Asymptotic expansion of Feynman integrals near threshold*, *Nucl. Phys. B* **522** (1998) 321 [[hep-ph/9711391](#)] [INSPIRE].
- [39] G. Passarino and M.J.G. Veltman, *One Loop Corrections for e^+e^- Annihilation Into $\mu^+\mu^-$ in the Weinberg Model*, *Nucl. Phys. B* **160** (1979) 151 [INSPIRE].
- [40] P. Mastrolia, T. Peraro and A. Primo, *Adaptive Integrand Decomposition in parallel and orthogonal space*, *JHEP* **08** (2016) 164 [[arXiv:1605.03157](#)] [INSPIRE].
- [41] T. Peraro, *Scattering amplitudes over finite fields and multivariate functional reconstruction*, *JHEP* **12** (2016) 030 [[arXiv:1608.01902](#)] [INSPIRE].
- [42] T. Peraro, *FiniteFlow: multivariate functional reconstruction using finite fields and dataflow graphs*, *JHEP* **07** (2019) 031 [[arXiv:1905.08019](#)] [INSPIRE].
- [43] W.H. Furry, *A Symmetry Theorem in the Positron Theory*, *Phys. Rev.* **51** (1937) 125 [INSPIRE].
- [44] L. Chen and M. Czakon, *Renormalization of the axial current operator in dimensional regularization at four-loop in QCD*, *JHEP* **01** (2022) 187 [[arXiv:2112.03795](#)] [INSPIRE].
- [45] T. Gehrmann and A. Primo, *The three-loop singlet contribution to the massless axial-vector quark form factor*, *Phys. Lett. B* **816** (2021) 136223 [[arXiv:2102.12880](#)] [INSPIRE].
- [46] S. Catani, *The Singular behavior of QCD amplitudes at two loop order*, *Phys. Lett. B* **427** (1998) 161 [[hep-ph/9802439](#)] [INSPIRE].
- [47] T. Becher and M. Neubert, *On the Structure of Infrared Singularities of Gauge-Theory Amplitudes*, *JHEP* **06** (2009) 081 [[arXiv:0903.1126](#)] [INSPIRE].
- [48] L.J. Dixon, E. Gardi and L. Magnea, *On soft singularities at three loops and beyond*, *JHEP* **02** (2010) 081 [[arXiv:0910.3653](#)] [INSPIRE].
- [49] F. Cascioli, P. Maierhöfer and S. Pozzorini, *Scattering Amplitudes with Open Loops*, *Phys. Rev. Lett.* **108** (2012) 111601 [[arXiv:1111.5206](#)] [INSPIRE].
- [50] F. Buccioni et al., *OpenLoops 2*, *Eur. Phys. J. C* **79** (2019) 866 [[arXiv:1907.13071](#)] [INSPIRE].

- [51] J. Currie, T. Gehrmann, A. Huss and J. Niehues, *NNLO QCD corrections to jet production in deep inelastic scattering*, *JHEP* **07** (2017) 018 [[arXiv:1703.05977](#)] [[INSPIRE](#)].
- [52] L. Chen, M. Czakon and M. Niggetiedt, *The complete singlet contribution to the massless quark form factor at three loops in QCD*, *JHEP* **12** (2021) 095 [[arXiv:2109.01917](#)] [[INSPIRE](#)].
- [53] T. Gehrmann, E.W.N. Glover, A. Huss, J. Niehues and H. Zhang, *NNLO QCD corrections to event orientation in e^+e^- annihilation*, *Phys. Lett. B* **775** (2017) 185 [[arXiv:1709.01097](#)] [[INSPIRE](#)].